EUROPEAN ORGANISATION FOR NUCLEAR RESEARCH
European Laboratory for Particle Physics

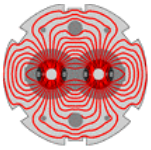

Large Hadron Collider Project

LHC Project Report 307

Surface Resistance Measurements and Estimate of the Beam-Induced Resistive Wall Heating of the LHC Dipole Beam Screen

F. Caspers, M. Morvillo, F. Ruggiero and J. Tan

Abstract

An estimate of the resistive losses in the LHC beam screen is given from cold surface resistance measurements using the shielded pair technique, with particular emphasis on the effect of a high magnetic field. Two different copper coating methods, namely electro-deposition and co-lamination, have been evaluated. Experimental data are compared with theories including the anomalous skin effect and the magneto-resistance effect. It is shown that whether the theory underestimates or not the losses depends strongly on the RRR value, on the magnetic field and on the surface characteristics. In the pessimistic case and for nominal machine parameters, the estimated beam-induced resistive wall heating can be as large as 260 mW/m for two circulating beams.

SL Division
PS Division

Administrative Secretariat
LHC Division
CERN
CH-1211 Geneva 23
Switzerland

Geneva, 23rd August 1999

Surface Resistance Measurements and Estimate of the Beam-Induced Resistive Wall Heating of the LHC Dipole Beam Screen

F. Caspers, M. Morvillo, F. Ruggiero and J. Tan*, CERN, Geneva, Switzerland

1 Introduction

The present technical choice for the LHC beam screen is a stainless steel (SS) beam pipe with a 50 μm copper coating on its inner surface [1]. The parasitic power dissipation per unit length in a circular beam screen is given by :

$$\frac{P}{L} = \frac{I_{av}^2 \cdot c^2}{M \cdot f_0 \cdot \pi} \int_0^\infty \left|\tilde{\lambda}(\omega)\right|^2 \cdot \frac{R_s(\omega)}{l} \cdot d\omega \quad [\mathrm{W/m}], \tag{1}$$

where I_{av} is the average beam current, M the number of bunches, f_0 the revolution frequency, c the velocity of light, $R_s(\omega)$ the surface resistance, l the perimeter of the beam screen cross section, $\tilde{\lambda}(\omega)$ the bunch spectrum and ω the angular frequency. In the classical regime, the surface resistance is:

$$R_s(\omega) = \sqrt{\frac{\omega \mu_0 \rho}{2}} \ [\Omega], \tag{2}$$

where ρ is the resistivity. The anomalous skin effect theory [2] takes into account the reduction of the skin depth δ at high frequencies if compared to the mean free path length λ of the conduction electrons at low temperature. An interpolation formula predicts :

$$R_s(\omega) = R_\infty \left(1 + 1.157\alpha^{-0.276}\right), \text{ for } \alpha \geq 3, \tag{3}$$

where $\alpha = \frac{3}{2}\left(\frac{\lambda}{\delta}\right)^2 = \frac{3}{4}\omega\mu_0(\rho\lambda)^2\rho^{-3}$ is dimensionless. The physical meaning of R_∞ is :

$R_\infty = \left(\frac{\sqrt{3}}{16\pi}\rho\lambda(\omega\mu_0)^2\right)^{\frac{1}{3}} = 1.123\times10^{-3}\left(\frac{\omega}{2\pi\ \mathrm{GHz}}\right)^{\frac{2}{3}}$, and is expressed in [Ω].

Owing to magneto-resistance, the resistivity may be described by the Kohler law [3]:

$$\rho_{B,T} = \rho_0(T) \times \left(1 + 10^{1.055 \cdot \log(B \times RRR) - 2.69}\right). \tag{4}$$

where B is the magnetic field in Tesla and $\rho_0(T)$ the resistivity at temperature T in the absence of magnetic field. As the resistivity decreases with temperature towards a minimum, the *RRR* which stands for the Residual Resistance Ratio, is defined as the ratio of the dc resistivity at room temperature to its cold-dc lower limit. Assuming $\rho_0(20\mathrm{K}) = 1.55\cdot10^{-10}$ Ω·m, RRR = 100 and B = 8.386 T, one finds $\rho_{B,T} = 5.39\cdot10^{-10}$ Ω·m.

* e-mail: jocelyn.tan@cern.ch

For a Gaussian bunch with r.m.s. bunch length of 7.5 cm, the classically computed value of the beam-induced resistive wall heating of the LHC beam screen with radius of 17.4 mm, at top energy and for nominal beam parameters (I_{av} = 0.56 A), is 82 mW/m/beam. On one hand, the theoretical estimate should be 12% higher when the anomalous skin effect is taken into account. On the other hand the figures raised at up to 70% referring to measurements of the SSC beam tube [4]. The discrepancy between these data motivated the RF impedance measurement programme initiated in 1995 [5]. First measurements at room temperature and liquid helium temperature were performed on copper electro-plated tubes [6]. These confirmed that the theory had underestimated the beam-induced resistive wall heating.

The present note is a follow-up of the previous campaign, and compares surface resistance data from two tubes with different coating techniques. In addition, measurements were performed in a high magnetic field by placing the experimental set-up in a superconducting dipole.

2 Experimental set-up

2.1 Principles and procedures

The measurement principle is based on the so-called shielded pair technique [7], which consists of a one metre long cylindrical TEM cavity with two cylindrical inner conductors (see Figure 1). A detailed description of the experimental set-up is given in ref. [6]. Basically, processing of the loaded quality factors measured in the even and odd mode excitations, in steps of ~150MHz, yields the surface resistance of the outer tube and of the inner conductors, assuming that the latter have an identical copper coating.

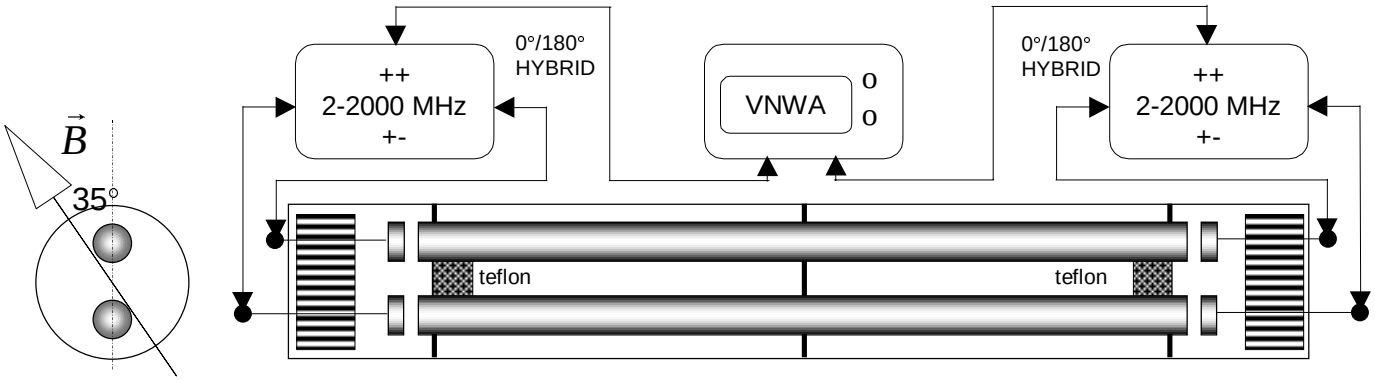

Figure 1: Cross section and side view of the experimental setup: a vector network analyser (VNWA) is used in conjunction with two hybrids, yielding either even (++) or odd (+-) mode excitation for a 1 m long cylindrical cavity with 2 inner conductors, held by 3 Teflon supports. The near degeneracy of even and odd modes is removed by 2 teflon blocks (splitters) placed between the inner conductors.

Then the resonator is placed in a vacuum tight tube inserted in the magnet pipe. The tube is electrically insulated with kapton tape. The magnetic field lines form an angle of about 35° with respect to the plane of the two inner conductors (see cross section in Figure 1), which also corresponds to the plane where the current flows. The coupling between the cavity and the external circuit is adjusted by changing the position of the two coupling networks. The coupling is set equal for the two ports before the cavity is mounted because it cannot be

changed once the system is inside the cryostat. The coupling is adjusted at the lowest level that allows us measuring the loaded Q of all modes with a good precision.

Once the magnet is installed in the cryostat, the system is pumped down to about 10^{-5} mbar and cooled down to 1.8 K. An important issue for the soundness of the measurements is to ensure that the whole resonator is at 1.8 K. The first test performed at 4.2 K had proved the mechanical contact between the resonator and the tube was not sufficient to cool down the resonator in a reasonable time. The problem was even worse for the inner conductors as they are very well thermally insulated by the teflon supports. In addition, no thermometer can be placed on them. The problem is solved by injecting a small quantity of helium in the system. This cools down the whole resonator in a few seconds. After injection the loaded Q raises suddenly.

2.2 Resonator preparation

Two outer tubes are prepared with different coating techniques [8]. The first one is a 304L SS tube electro-plated then annealed at 300°C (one hour under vacuum) to allow grain growth. Thereafter, the RRR is equal to 217. Micrographs in Figure 2 reveal pyramidal-shaped structures of 10-15 μm height. The average roughness is 2.53 μm in either longitudinal ($R_a^{//}$) and transverse ($R_a^{\perp}$) directions. The two inner conductors have been treated the same way.

The second outer tube is made of two sheets, one of SS Ugine UNS 21904 grade and one of copper, co-laminated in the *longitudinal* direction. Before being rolled to form a tube, the co-laminated sheet was annealed at 920°C for 6 min under H_2 atmosphere. This process should ensure a good interdiffusion process at the copper-steel interface. The annealing time is an important parameter as the RRR of co-laminated copper is affected by two phenomena : i/ up to 3 mn, annealing and possibly recrystallisation tend to decrease the residual resistivity; ii/ afterwards diffusion of SS alloy elements (Ni, Cr, Mn…) into copper, which can be likened as a poisoning effect, increases the residual resistivity. The RRR values on flat sheet are around 100. The cold deformation of the copper during the tube forming process reduces the RRR value down to 60. Figure 3 shows details of the copper rolled surface, characterized by longitudinal grooves, parallel to the rolled direction. The co-laminated technique results in a smoother surface than the electro-plated one, with $R_a^{\perp} = 0.39$ μm and $R_a^{//} = 0.16$ μm. Note that $R_a^{\perp}$ is ~ 2.4 times larger than $R_a^{//}$.

a/

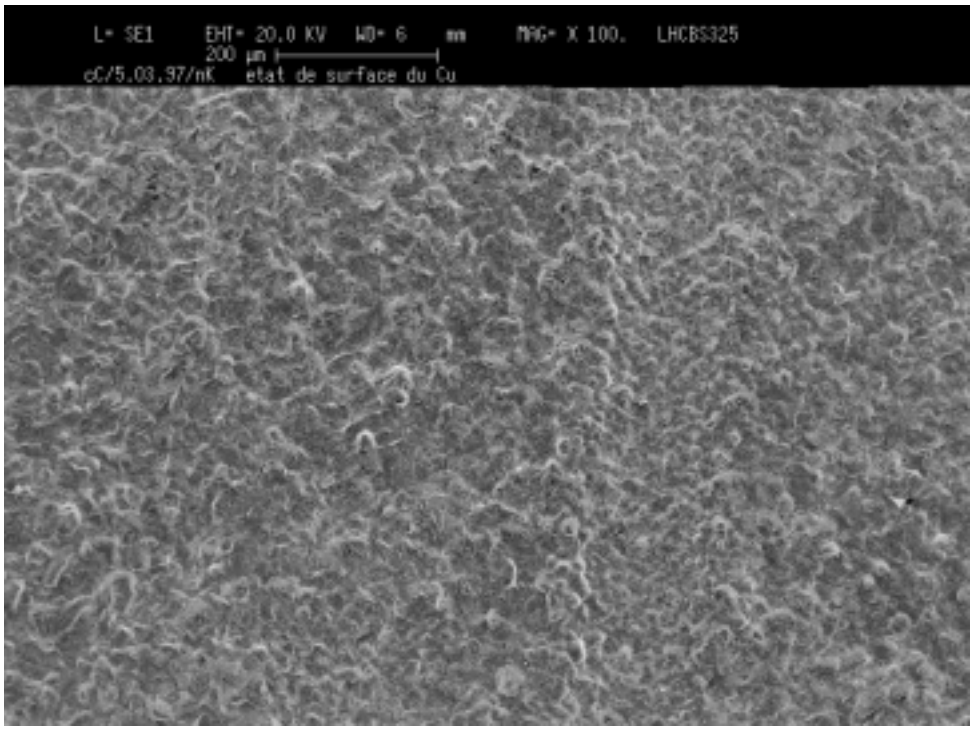

b/

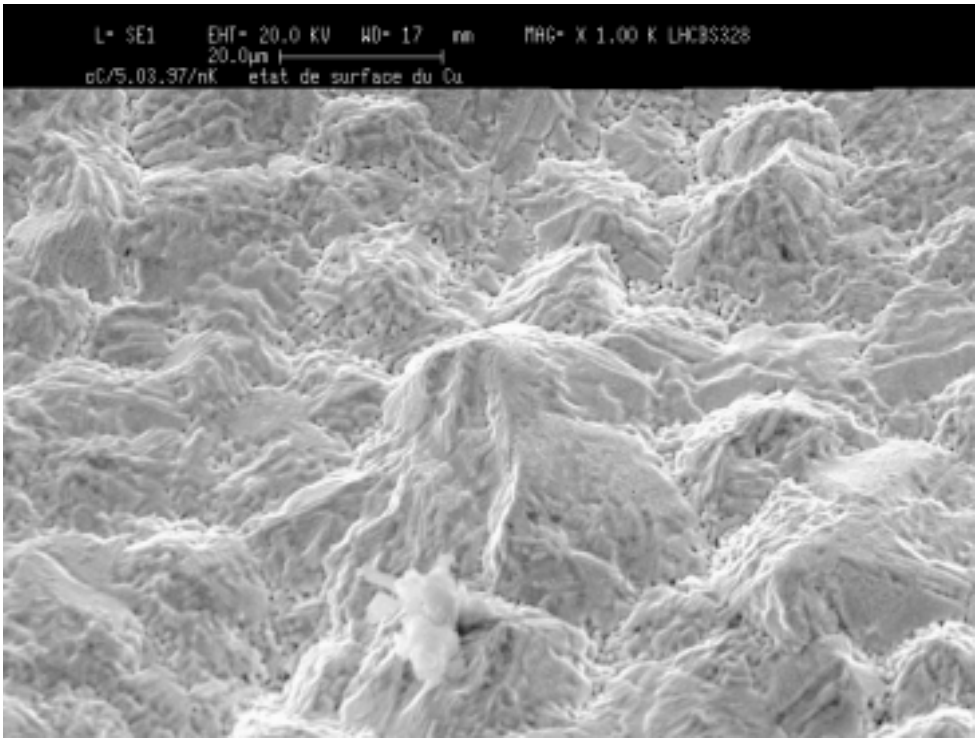

Figure 2 : *SEM micrographs of the electro-plated copper coating. a/ Magnification ×100; b/ Magnification ×1000 and surface tilted at 45°.* $R_a^{\perp}$ *= 2.52 µm and* $R_a^{//}$ *= 2.53 µm (from [8]).*

a/

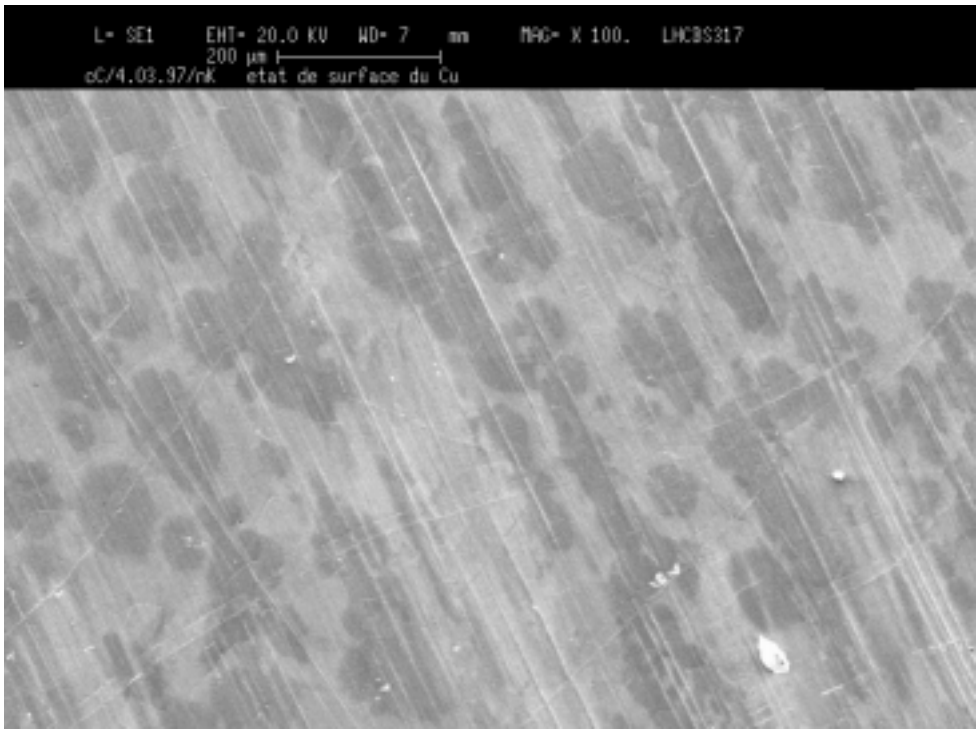

b/

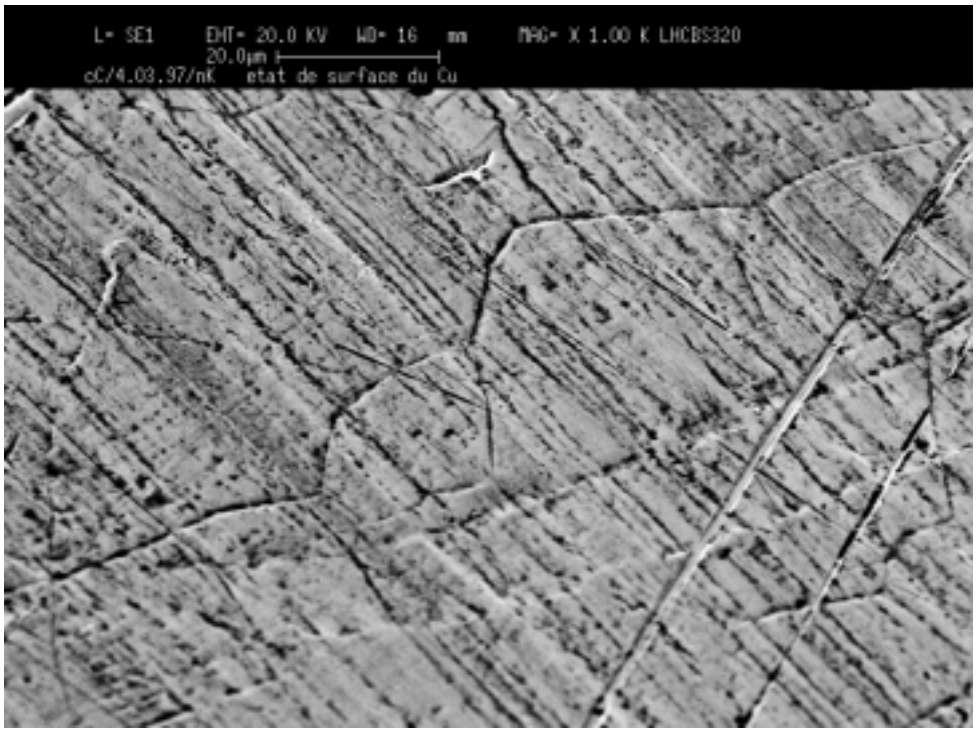

Figure 3: SEM micrographs of the co-laminated copper coating. a/ Magnification ×100; b/ Magnification ×1000 and surface tilted at 45°. $R_a^{\perp}$ = 0.39 µm and $R_a^{//}$ = 0.16 µm (from [8]).

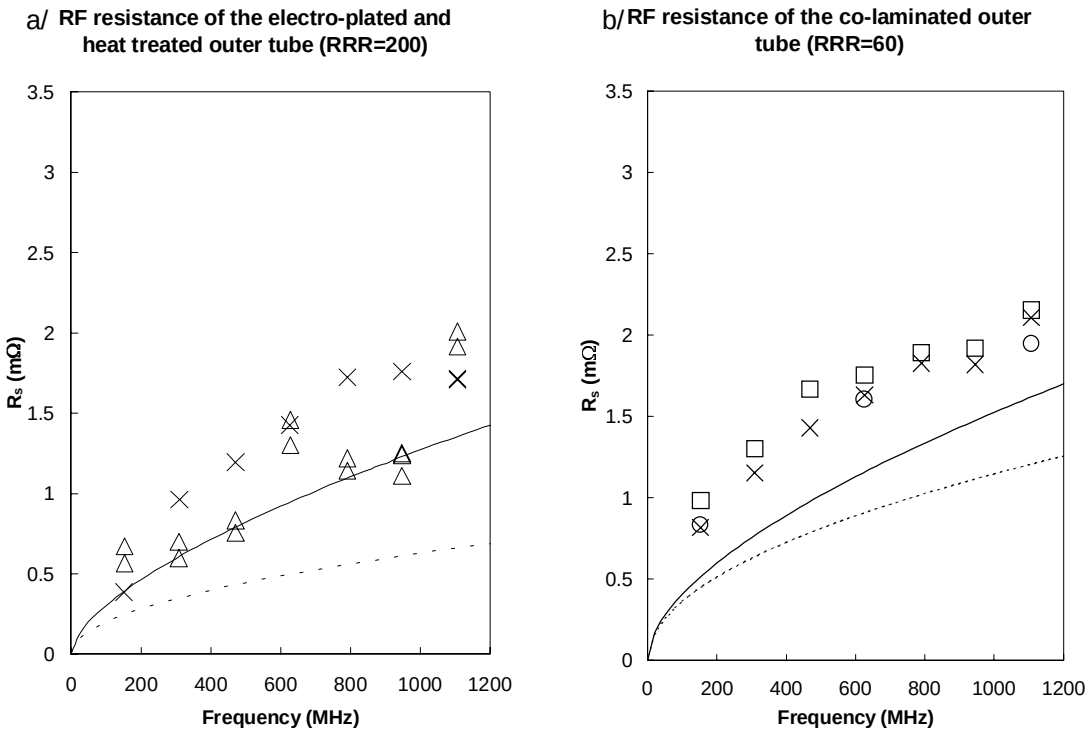

Figure 4: Surface resistance measured at liquid Helium temperature of the outer tube with two copper coating techniques : a/ electro-plated + heat treated, and b/ co-laminated. Crosses refer to measurements without B field while triangles, circles and squares refer to measurements performed with 8.3 T, 2.21 T and 8.47 T, respectively. The predictions without magnetic field in the classical (dashed line) and the anomalous regimes (solid line) are added assuming $\rho_0(300K) = 1.55\times10^{-8}\Omega.m$.

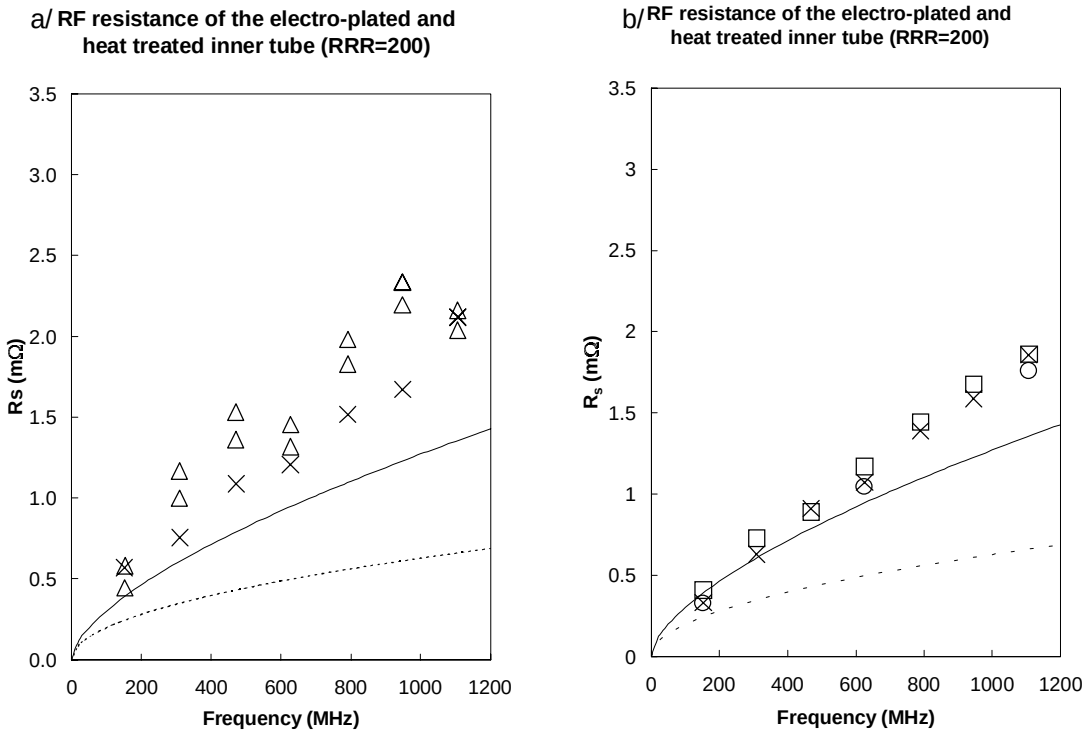

Figure 5: Cold surface resistance measurements of the inner conductors with the following configurations: a/ with the electro-plated outer tube, and b/ with the co-laminated outer tube. Same legends are used as in the previous figure.

3 Experimental results

Figure 4 compares the surface resistance measurements of electro-plated (Figure 4a) and co-laminated (Figure 4b) outer tubes vs frequency and vs B field. Results for the inner conductors are also presented in the next figure, when the electro-plated outer tube is used (Figure 5a), and when the co-laminated outer tube is used (Figure 5b). The dashed lines and the solid lines represent the predictions in the classical and anomalous theory respectively.

Though yielding different RRR values, data without B field from both outer tubes are close to each other. Note in this case the good reproducibility of surface resistance curves for the inner conductors. Further this parameter is slightly affected by the application of a low magnetic field (plots with circles).

However, the surface resistance of the co-laminated outer tube is ~ 7.5 - 9% larger when operating with high magnetic field (plots with squares). The electro-plated outer tube configuration exhibits an oscillating trend versus frequency. It also should be noted that a maximum peak of R_s for the outer tube (Figure 4a) corresponds to a minimum of R_s for the inner conductors (Figure 5a) and vice versa. When the latter are used in conjunction with the co-laminated outer tubes this behaviour is strongly damped. This effect is being investigated by new measurements, both cold and at room temperature, and the results will be discussed in a future technical report. Ripples in the curves of Q versus frequency may be due to :

1. localised defects, such as scratches observed on the coated surface and emphasized by strong magnetic fields. The measured Q's from which R_s^{inn} and R_s^{out} are deduced may be perturbated by these defects;
2. dielectric losses in the centre support where the electric field is maximum for even harmonic numbers. However this effect should be very minor as the $tan(\delta)$ of teflon amounts to 10^{-4};
3. some residual mode coupling. While measuring the Q factors in a given mode excitation (odd or even), a residual resonance peak is sometimes observed : in this case one may loose some power to the undesired mode and this coupling depends on the presence of an electric field at the centre disk (even harmonic numbers).

Figure 6 shows the variation of the loaded Q for a given mode versus magnetic field. As the quality factor is inversely proportional to the losses in the cavity walls, the curve is interpreted as an initial lowering of the surface resistance to a minimum which occurs at ~ 1.85 T. Beyond this value, the surface resistance starts to increase. These observations are consistent with measurements at 2.21 T, represented by the plots with circles of Figure 4b and of Figure 5b where the resistance values are smaller than those without B field and curves with strong B field.

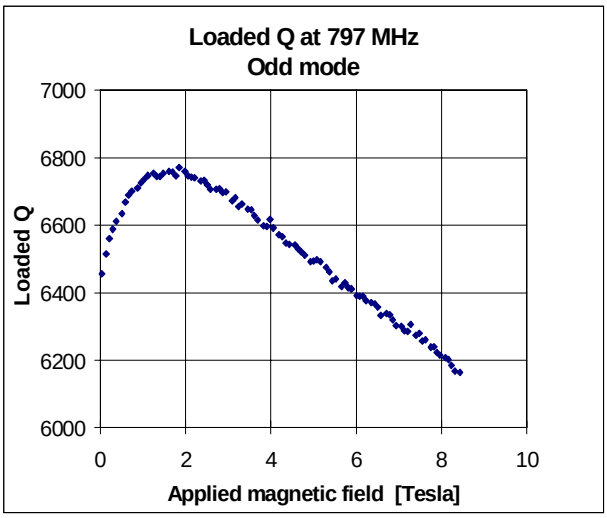

Figure 6: Variation of the loaded Q (odd mode) versus B field. Data were obtained with the co-laminated cavity, during B field rising from 0.4 to 8.43 T, with a rate of 0.15 T/s, and data acquisition each 5 seconds.

4 Discussion

The variation of the RF impedance with magnetic field had been already reported by J.T. Rogers et al. [9]. They could observe an initial decrease of R_s saturating in the range 2-3 Tesla followed by an increase of surface resistance, quadratically in the B field. The authors concluded that at the saturation value "*the cyclotron radius is of the same order as the mean free path and skin depth. This is consistent with the assumption that the magnetic field decreases the rate of collisions with the surface and that the resultant increase in conductivity is due to the finite size of the RF conduction layer*". It has also been shown that R_s varies with the field direction. Indeed, the longitudinal magneto-resistance is, in general smaller than the transverse magneto-resistance. In the present work, the orientation of 35° choosen for the magnetic field is a compromise between the two extrema.

On the basis of the results presented in this paper, some fits were performed, including a large number of parametres which could affect the surface resistance : RRR, magneto-resistance, frequency and material. It was empirically found that the main changes in the anomalous resistance formula in Eq. (3) occur at the prefactor and the power of α. This gives a modified law for large RRR (typically 200) :

$$RRR = 200 \quad \begin{cases} R_s'(\omega) = R_\infty\left(1 + 1.05\alpha^{-0.1}\right) & \text{if } B = 0 \\ R_{s,B}'(\omega) = R_\infty\left(1 + 0.75\alpha^{-0.1}\right) & \text{if } B \neq 0 \end{cases}$$

For small RRR (60 here), one finds :

$$RRR = 60 \quad \begin{cases} R_s''(\omega) = R_\infty\left(1 + 7.72\alpha^{-0.46}\right) & \text{if } B = 0 \\ R_{s,B}''(\omega) = R_\infty\left(1 + 2.55\alpha^{-0.46}\right) & \text{if } B \neq 0 \end{cases}$$

These relations were used in Eq. (1) to compute the parasitic power dissipation per unit length and per beam. Table 1 compares the power contributions from the classical, anomalous, and the empirical laws.

	RRR = 60 co-laminated tube		RRR = 200 electro-plated tube	
B [T]	0	8.386	0	8.386
$\rho_{B,T} \times 10^{10}$ [Ω·m]	2.58	6.31	0.77	4.77
$P_{classical}$ /L [mW/m/beam]	57	88	31	77
$P_{anomalous}$ /L [mW/m/beam]	74	96	61	87
$P_{empirical}$ /L [mW/m/beam]	**120**	**129**	**80**	**86**
$\frac{P_{empirical}}{P_{anomalous}}$	1.62	1.34	1.31	0.988

Table 1: Relevant parameters and power loss estimates in the LHC dipole beam screen owing to surface resistance in the classical, anomalous and empirical regimes. The figures which refer to the latter are deduced from our measurements and are typed in bold . One assumes $\rho_0(300K) = 1.55 \times 10^{-8}$ *Ω·m.*

According to the experimental data, the magneto-resistance contribution to the heat load is ~ 8% whatever the coating method. In the pessimistic case where RRR = 60, the increase reaches a top of 129 mW/m/beam for nominal machine parameters, which is 34% larger than the value predicted by the anomalous skin effect theory. In only one case where RRR = 200, the prediction of 87 mW/m/beam fits with the measurements. It appears also that the co-lamination process yields larger losses than the electro-plating one : +50% with or without magnetic field, yet lower than the square root of the RRRs' ratio = $\sqrt{200/60}$ ~1.82 providing an expected relative increase of 82%. The descrepancy may be related to the surface roughness resulting from the cladding method.

In Eq. (1), the product $c^2 \cdot \left|\tilde{\lambda}(\omega)\right|^2 \cdot R_s(\omega) = \exp\left(-\frac{\sigma_z^2 \cdot \omega^2}{c^2}\right) \cdot R_s(\omega) \equiv p(\omega)$ which represents the function to be integrated is also plotted versus frequency (see Figure 7a-d). The three curves in each figure show the variation computed in the classical, anomalous and empirical regimes respectively . The four figures refer to the different experimental configurations (RRR and B field). Here, the areas are related to the losses whose major weight mainly occurs at relatively low frequencies, as the gaussian bunch spectrum extends up to 637 MHz, r.m.s.

In a relevant work devoted to precise measurements of dissipation factor in microwave printed circuit boards [10], Tanaka and Okada had compared the effective conductivity of rolled copper foil and of electro-deposited copper foil having similar dc conductivities at room temperature, in the range $5.3\text{-}5.5 \times 10^7$ $S.m^{-1}$. The authors showed that the conductivity at 10 GHz increases as R_a decreases and rapidly approaches the value of dc conductivity. They measured the conductivity in the microwave regime from 1 to 25 GHz, and found higher values for the rolled copper than for the electro-plated copper, slowly decreasing as the frequency increased. Furthermore, they demonstrated experimentally that rolled copper

conductivity exhibited anisotropic characteristics. Although $R_a^{//}$ was lower than $R_a^{\perp}$, the conductivity in the rolled direction was unexpectedly larger than that in the perpendicular direction. This was interpreted in terms of the difference between the calculated R_a and the true one, owing to submicron features like bending pits or wide holes with narrow entrances which cannot be measured by usual surface-roughness-meters.

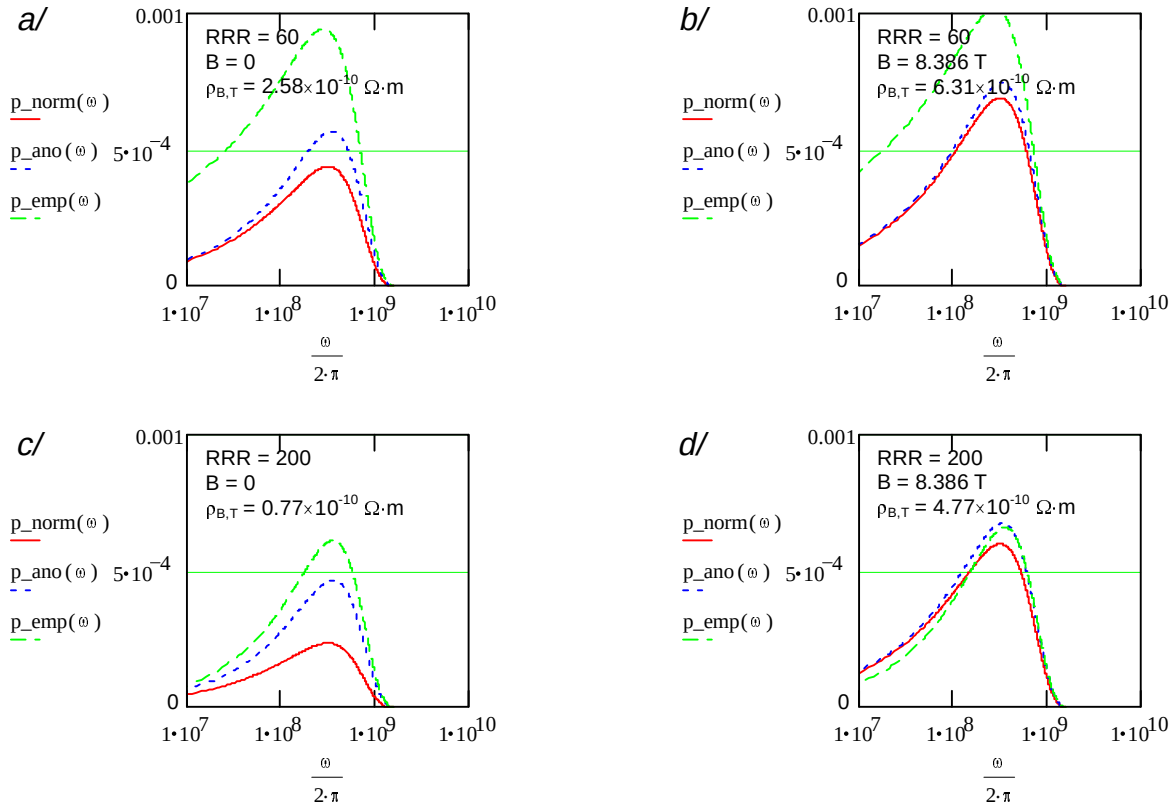

Figure 7: Relative weight of the power losses expressed by the product $c^2 \cdot \left|\tilde{\lambda}(\omega)\right|^2 \cdot R_s(\omega) \equiv p(\omega)$ *to be integrated in Eq. (1), versus frequency. The curves in solid lines, dashed lines and long-dashed lines represent the classical, anomalous and empirical regimes, respectively.*

With respect to the goal of the present paper, one may classify the phenomena that concurrently affect the dissipated power into two categories :

1. extrinsic parameters related to the working conditions such as the anomalous skin effect and the magneto-resistance effect which increase the losses,
2. intrinsic parameters related to the material such as the Residual Resistance Ratio and the cladding process which may limit the losses.

5 Conclusions and outlook

A surface resistance measurement programme using the shielded pair method has been undertaken to evaluate the surface resistive wall heating of the LHC beam screen. From the empirical use of the interpolation formula, it is possible to give a realistic estimate of the heat load owing to the anomalous skin effect and the magneto-resistance effect. On one hand, it is found that RRR-induced losses are larger than magnetic-field-induced losses. On the other hand, the calculated figures from the empirical law confirm that the theories had

underestimated the beam-induced wall heating as the submicron-scaled surface features were neglected. In the less favourable case, the surface heating can be as high as 130 mW/m per circulating beam.

The co-lamination process is being improved, using a new stainless steel, the P506 grade which is the final technical choice. Further, co-laminated sheets can undergo additional treatments such as ribbed structure, sawtooth shaped Cu surface in the median plane to reduce the reflectivity [11] and hence the photo-electron yield from the incoming synchrotron radiation.

New smooth tubes and ribbed tubes are being produced, and cold surface resistance measurements will be performed on either tube in the forthcoming months. In parallel, the resonator upgrade is under way to increase the working range up to 2.5 GHz and to lower undesired RF losses, as this device is very sensitive to mechanical tolerances. The technical solutions and final results will be described in a forthcoming report.

6 Acknowledgements

The authors are greatful to their colleagues for technical supports and for fruitfull discussions, namely :

C. Benvenuti and S. Sgobba of EST/SM group,

L. Nikitina and C. Reymermier of EST/ESM group,

G. Ferlin of LHC/ACR group,

A. Jacquemod and A. Poncet of LHC/CRI group,

S. Chevassus-à-l'Antoine and J.-M. Rieubland of LHC/ECR group,

A. Arn, J.-M Cottin, P. Viret and L. Walckiers of LHC/MTA group,

O. Gröbner and N. Kos of LHC/VAC group,

H. Tsutsui of SL/AP group.

References

1 The LHC Study Group, *The Large Hadron Collider, Conceptual Design*, CERN/AC/95-05 (LHC), 1995.

2 A.B. Pippard, *The surface impedance of superconductors and normal metals at high frequencies. II. The anomalous skin effect in normal metals*, Proc. Roy. Society (London), **A191**, 385, 1947.

3 M. Kohler, Ann. Physik, **Ser.5 32**, 211, 1938.

4 E.R. Gray, *SSC beam tube resistance measurements*, LANL Technical Note no AT-1:93-344, 1993.

5 W. Chou and F. Ruggiero, *Anomalous skin effect and resistive wall heating*, CERN LHC Project Note 2, 1995.

6 F. Caspers, M. Morvillo and F. Ruggiero, *Surface resistance measurements for the LHC beam screen*, LHC Project Report 115, 1997.

7 G.S. Smith and J.D. Nordgård, *On the design and optimization of the shielded-pair transmission line*, IEEE Trans. Microwave Theory and Tech., **MTT-28**, 887, 1980.

8 C. Campedel, *Comparison between different copper surface states*, CERN, Report EST/SM/MB 97/03/09, 1997.

9 J.T. Rogers, S. De Panfilis, A.C. Melissinos, B.E. Moskowitz, Y.K. Semertzidis, W.U. Wuensch, H.J. Halama, A.G. Prodell, W.B. Fowler and F.A. Nezrick, *Anomalous RF magneto-resistance in copper at 4 K*, University of Rochester/ Department of Physics and Astromony, UR1043, 1988 — Appl. Phys. Lett. **52**, 2266-2268, 1988.

10 H. Tanaka and F. Okada, *Precise measurements of dissipation factor in microwave printed circuit boards*, IEEE Trans. Instr. and Meas., **IM-38**, 509-514, 1989.

11 V. Baglin, O. Brüning, R. Calder, F. Caspers, I.R. Collins, O. Gröbner, N. Hilleret, J.-M. Laurent, M. Morvillo, M. Pivi and F. Ruggiero, *Beam-induced electron cloud in the LHC and possible remedies*, CERN, LHC Project Report 188, 1998.